Spectroscopy 16 (2002) 107–120
IOS Press

Dynamic aspect of bacteriorhodopsin as viewed from ^{13}C NMR: Conformational elucidation, surface dynamics and information transfer from the surface to inner residues

H. Saitô, R. Kawaminami, M. Tanio, T. Arakawa, S. Yamaguchi and S. Tuzi
Department of Life Science, Himeji Institute of Technology, Harima Science Garden City, Kamigori, Hyogo 678-1297, Japan

Abstract. We demonstrate here how dynamic as well as conformational features of bacteriorhodopsin (bR) in purple membrane (PM) as a typical membrane protein are revealed by extensive ^{13}C NMR studies on [3-^{13}C]-, [2-^{13}C]-, [1-^{13}C]Ala or [1-^{13}C]Val-labeled bR and a variety of site-directed mutants. A number of ^{13}C NMR peaks were well-resolved for [3-^{13}C]Ala- and [1-^{13}C]Val-bR under the condition of fully hydrated PM at ambient temperature and assigned to individual amino-acid residues, initially by regio-specific manner with reference to the data of the conformation-dependent displacements of peaks from model polypeptides and subsequently by site-specific manner with reference to the specifically reduced peak-intensities of site-directed mutant as compared with those of wild type. It is noticeable that the revealed bR structure at ambient temperature by ^{13}C NMR is not static as anticipated from the data of diffraction studies at cryo-temperature but is dynamically heterogeneous undergoing motional fluctuations with various frequencies (10^2–10^8 Hz) depending upon the domains of interest. We further applied this approach to reveal how charged state of surface residues, especially at the side-chain of exracellular Glu residues (Glu 194 and 204), could be transmitted to the inner part of the helices such as Ala 53, 84, and 215 to alter their local conformations of transmembrane helices near at the Schiff base through side-chain interactions. We also analyzed how information of the protonation at Asp 85 from helix C is initially transmitted to helices B (Val 49) and G (Val 213) though modified helix-helix interactions through the side-chains of Arg 82.

1. Introduction

Determination of the three-dimensional (3D) structure of a variety of biological molecules such as proteins, biologically active peptides, nucleic acids, carbohydrates, etc. is undoubtedly very important to gain insight into their structure–function relationship. Even though X-ray crystallography and multidimensional NMR spectroscopy have proved to be the most favorable standard means to yield such 3D structures for these molecules in crystals and aqueous solution, respectively, these two approaches are not always straightforwardly applied to a variety of membrane proteins because of underlying problems such as difficulty in crystallization and increased linewidths caused by increased effective molecular mass due to the presence of oligomeric form instead of monomeric form as well as contribution of surrounding lipid molecules, respectively.

It is for this reason that the high-resolution solid-state NMR approach can be sought as a complementary means to be able to study the conformation and dynamics of a variety of membrane proteins, although suitable isotope enrichment by either ^{13}C or ^{15}N nuclei is essential to improve both *sensitivity* and

selectivity of particular residues of interest for recording spectra. In principle, detailed conformational aspect of these molecules can be obtained by careful analysis of anisotropic nuclear spin interactions in the solid such as chemical shift anisotropy and dipolar and quadrupolar interactions, if certain type of oriented samples to applied magnetic field is available [1,2]. This kind of approach, however, is inevitably limited to smaller peptide fragments rather than *whole* proteins by taking into account of the manner of sample preparations. Therefore, it is too premature to expect direct determination of 3D structure of intact membrane proteins by solid-state NMR as a similar manner to the current solution multidimensional NMR, because determination of sequential assignment of peaks as well as distance constraints is extremely difficult by solid state NMR in view of the current development of NMR methodology and more importantly dynamic aspect of a variety of membrane proteins [3].

Instead, we have explored an alternative but very simple approach to elucidate local conformation and dynamics of *intact* membrane proteins as demonstrated for extensive studies on bacteriorhodopsin (bR), known as a light-driven proton pump contained in the purple membrane (PM) of *Halobacterium salinurum* [4]. The chromophore of bR, retinal, is covalently linked to Lys216 through a protonated Schiff base. The photoisomerization of retinal from all-*trans* to 13-*cis* triggers a series of photocycle reactions, resulting in proton transfer from the cytoplasmic to the extracellular side of the membrane. The first proton transfer occurs from the protonated Schiff base to the anionic Asp85 in the L-to-M reaction [5]. Protonation of Asp85 induces the release of a proton from the proton release groups involving Glu194 and Glu204, and the deprotonation of Asp96, which causes proton uptake from cytoplasmic medium [6–8]. Revealed structures of the transmembrane α-helices either by cryo-electron microscopy or X-ray diffractions [9–12] are generally consistent but their surface structures are either obscured or inconsistent among them. One reason for this inconsistency of the surface structure may be that they are not always static but undergo motional fluctuations with various frequencies, as viewed from our recent ^{13}C NMR study [13]. In fact, we have recorded ^{13}C NMR spectra of ^{13}C-labeled intact bR and mutants and assigned a number of well-resolved ^{13}C NMR signals both from regio-specific and then site-specific manner, utilizing the available data base for the conformation-dependent displacement of ^{13}C NMR peaks [14–16], together with careful evaluation of reduced relative peak-intensities of site-directed mutants of interest with reference to the data of wild type.

In the present paper, we briefly outline our strategy including selection of the most appropriate manner of ^{13}C labeling, peak-assignment, dynamic aspect of bR at ambient temperature, so far obtained. Then, we demonstrate how this approach can be conveniently utilized as an effective means to analyze the manner of molecular mechanism of the information transfer from the extracellular surface to the inner part or vice versa through modified retinal-helix and helix–helix interactions including a plausible side-chain interactions among residues involved.

2. Preparation of ^{13}C-labeled proteins, ^{13}C NMR measurements, and assignment of peaks

Isotopically labeled bR samples needed for NMR studies are readily available from the large-scale culture of *H. salinurum* S-9 strain using synthetic media in which certain unlabeled amino acids were replaced with ^{13}C-labeled ones such as [1-^{13}C]Ala, Val, [2-^{13}C]Ala, or [3-^{13}C]Ala, as indicated in the circled (Ala) or boxed (Val) residues in the schematic representation of the primary structure of bR, taking into account of the secondary folding on the basis of X-ray diffraction [11] as shown in Fig. 1. Selective isotope labeling in this way could be most favorable in terms of achievement of the maximum sensitivity enhancement free from additional broadening due to scalar ^{13}C–^{13}C couplings, as compared

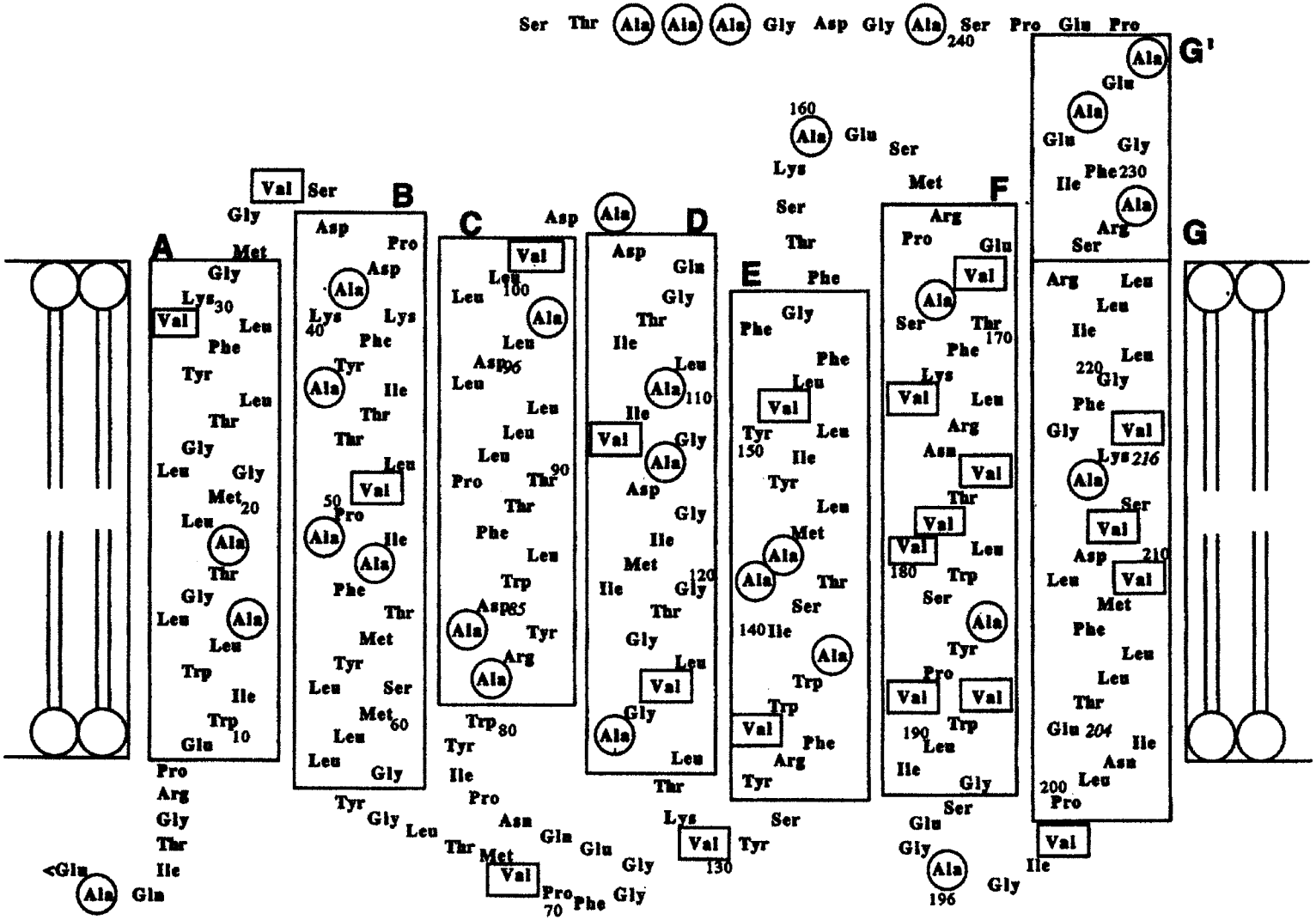

Fig. 1. Primary structure of bR taking into account of the secondary folding on the basis of X-ray diffraction [11]. All Ala and Val residues labeled by [^{13}C]Ala and [1-^{13}C]Val residues are indicated by the circles and boxes, respectively.

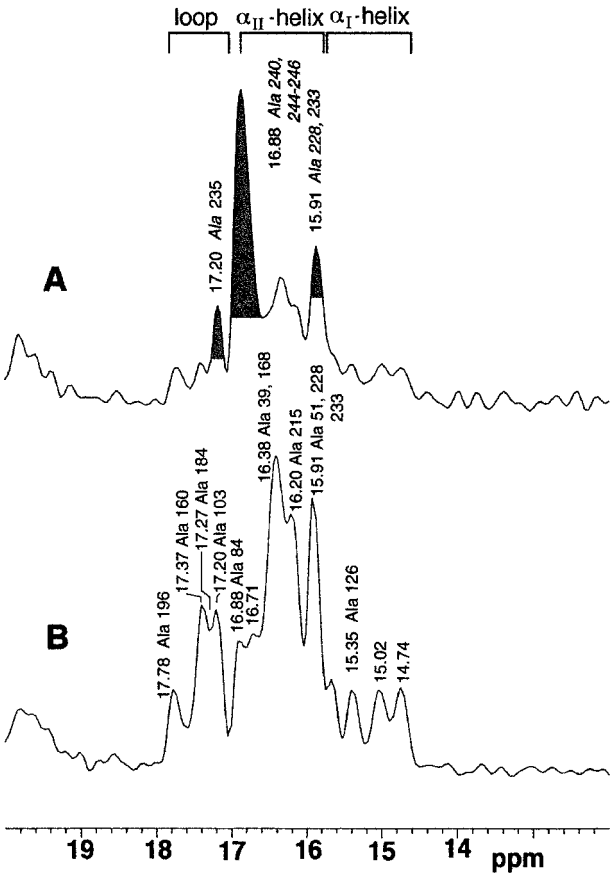

Fig. 2. ^{13}C DD-MAS (A) and CP-MAS (B) NMR spectra of [3-^{13}C]Ala-labeled bacteriorhodopsin. The ^{13}C NMR signals from the C terminal residues are in gray.

with the uniform or multiple labeling techniques currently available in solution NMR. A variety of site-directed mutants are also available from *H. salinurum* after transformation of shuttle vector coding the site-directed mutation. The pelleted preparations of centrifuged purple membrane were contained in a 5 mm o.d. sample rotor, tightly sealed with glue.

Figure 2 illustrates the ^{13}C NMR spectra of [3-^{13}C]Ala-labeled bR at ambient temperature, recorded by both dipolar decoupled magic angle spinning (DD-MAS) (A) and cross polarization-magic angle spinning (CP-MAS) (B), respectively [18]. Twelve ^{13}C NMR peaks, including the five single carbon signals among 29 Ala residues in bR, are well-resolved under the condition of excess hydration (Fig. 2). The three intense ^{13}C NMR signals marked by gray in the DD-MAS NMR spectrum (Fig. 2A) are suppressed in the corresponding CP-MAS spectrum (Fig. 2B), although the spectral features of the rest are unchanged. This is obviously caused by the presence of rapid motional fluctuations with correlation times shorter than the order of 10^{-8} s in the C- or N-terminal region protruded from the membrane surface. The regio-specific assignments of these peaks to either α-helices or loops can be made with reference to the data of the conformation-dependent ^{13}C chemical shifts of the C_α , C_β and C=O peaks, irrespective of their amino-acid sequences [3,14–17]. Site-directed assignment of the resolved peaks to individual amino-acid residues have been performed by locating the reduced peak of site-directed mutants which lack the amino acid residue of interest as compared with wild type. More than 60% of the

^{13}C NMR signals of [3-^{13}C]Ala residues in bR have been assigned by this procedure [3,19], as indicated on the top of individual peaks in Fig. 2. It is emphasized here that this kind of [3-^{13}C]Ala-labeling is the most suitable for a variety of membrane proteins in view of the achieved spectral resolution, the least possibility of isotope scrambling to other amino-acid residues [20] and of overlapping signals with those of natural abundance.

In contrast, it is expected that ^{13}C CP-MAS NMR spectral feature of [1-^{13}C] or [2-^{13}C]Ala-labeled bR is not always similar with that of DD-MAS technique as in the case of [3-^{13}C]Ala-bR, because ^{13}C NMR peaks from the transmembrane α-helices with longer spin-lattice relaxation times (T_1) in the order of 10 s could not effectively be detected by DD-MAS method, whereas ^{13}C NMR peaks of the residues located at the C-terminal tail or loops with rather shorter T_1 in the order of 1–0.5 s [13] could be selectively detected by DD-MAS and CP-MAS technique. Nevertheless, it turned out that no ^{13}C NMR signals from [1-^{13}C] or [2-^{13}C]Ala residues located at the loops or their vicinity were detected by both CP-MAS and DD-MAS techniques, because these signals were substantially broadened to the extent beyond recognition because of failure of attempted peak-narrowing by MAS technique caused by interference of incoherent frequency for the internal motions in the order of 10^{-4} s with coherent frequency of the magic angle spinning, as far as fully hydrated preparations were utilized [19]. Further, we found that ^{13}C NMR signals of [1,2,3-^{13}C]-bR gave rise to too broad ^{13}C NMR signals which are not any more useful as probes due to accelerated relaxation rate through multiple relaxation pathways [19].

It is noteworthy that ^{13}C NMR signal of [1-^{13}C]Val-labeled bR can be utilized as a suitable alternative probe for structural study of bR, as demonstrated for ^{13}C CP-MAS (left) and DD-MAS (right) NMR spectra of bR (Fig. 3A) and V101A mutant (Fig. 3B), respectively. The assignment of peaks was performed so far based on comparative studies on appropriate site-directed mutants V199A and V49A [21], and V179M, V213A, V187L, V217A (manuscript in preparation) and V101A and wild type, as indicated upon the top of the individual peaks by roman. In particular, the assignment of Val 101 peak to the peak at 171.0 ppm which is already assigned to Val 199 [21] can be confirmed in view of the reduced peak-intensity in the DD-MAS NMR spectrum of V101A mutant (Fig. 3B, right trace). Tentatively assigned peaks such as Val 130 and 34 are shown by italic, although further experimental confirmation using V130G and V34G mutants is now under way. It is noteworthy that ^{13}C NMR signals from the loops are now visible in the ^{13}C NMR spectra of [1-^{13}C]Val-labeled bR, in contrast to the case of [1-^{13}C]Ala-labeled preparation [13]. This is the reason why [1-^{13}C]Val-probe can be utilized as a more suitable probe both for the transmembrane α-helices and loops to yield well resolved peaks in the CP-MAS NMR spectra, whereas ^{13}C NMR signals from the loops are visible by the DD-MAS spectra alone. The present observation suggests that there appears a distinct change in the ^{13}C NMR spectral behavior between Ala and Val residues in response to such low frequency motion responsible for suppression of peaks (in the order of 10^{-4} s) as manifested from the distinct behavior mentioned above. In fact, it appears that such fluctuation motion may be hindered in the presence of more bulky side-chain at the C_α position as in Val residue.

3. Conformation and dynamic aspect of bR at ambient temperature

It is now feasible to discuss the local conformation and dynamic aspect of bR *at ambient temperature*, on the basis of the so far assigned peaks for [3-^{13}C]Ala- and [1-^{13}C]Val-bR as illustrated in Figs 2 and 3, respectively. In general, the present finding is consistent with the data of the secondary structures available from the previous diffraction data. Nevertheless, several new findings available only by the current

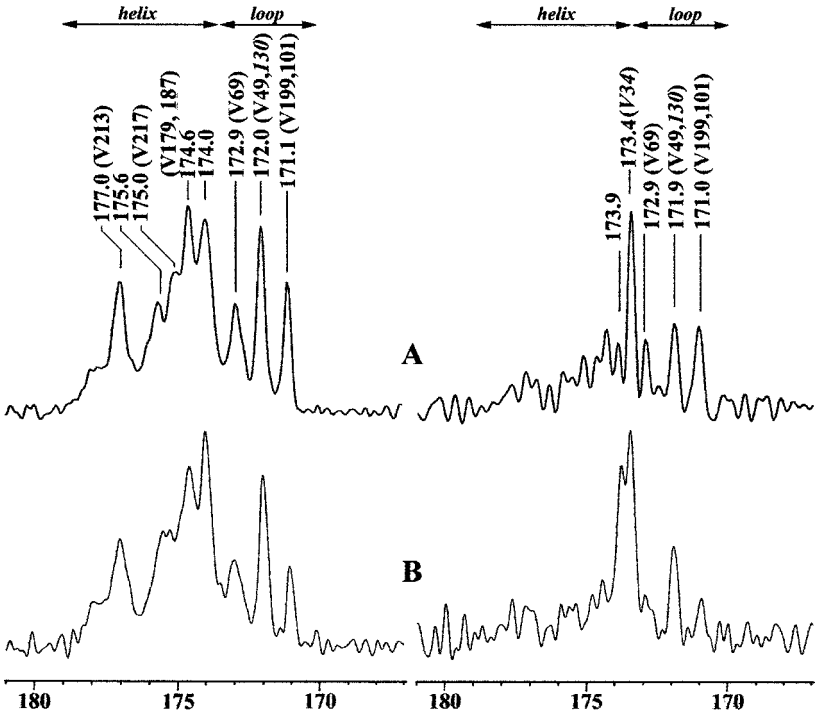

Fig. 3. ^{13}C CP-MAS (left) and DD-MAS (right) NMR spectra of [1-^{13}C]Val-labeled wild type (A) and V101A mutant (B) of bacteriorhodopsin.

^{13}C NMR study at ambient temperature are noteworthy. First, the presence of an α-helical segment at residues 226–235 is easily located from the conformation-dependent peak-position at 15.91 ppm which is characteristic of the α-helix and ascribable to Ala 228 and 233 [22,23]. This C-terminal α-helix (designated as G′) is anchored at the membrane surface and undergoes anisotropic fluctuation with correlation time in the order of 10^{-6} s as judged from the carbon spin–lattice relaxation times [3]. Second, it is noteworthy that many ^{13}C NMR signals from bR, as well as its transmembrane peptides incorporated into lipid bilayer [24], are displaced appreciably downfield by 0.3–1.5 ppm, depending upon particular amino acid sequence to the peak-positions of $\alpha_{\rm II}$-helix with reference to the ^{13}C chemical shift of $(Ala)_n$ in hexafluoroisopropanol (HFIP) solution according to the definition of Krimm and Dwivedi proposed for interpretation of infrared spectra [25]. Nevertheless, it turned out that ^{13}C NMR peaks of these peptides either in HFIP solution or cast preparation are resonated at the normal peak-position ($\alpha_{\rm I}$-helix) of the Ala C_β ^{13}C chemical shift of $(Ala)_n$ in the solid. This finding indicates that the presence of the $\alpha_{\rm II}$-helix as viewed from ^{13}C NMR data of [3-^{13}C]Ala-bR can be explained in terms of local conformational fluctuation (10^2 Hz) deviated from that of standard α-helix under anisotropic environment. In this connection, it seems to be more realistic to interpret the variation of in the ^{13}C chemical shifts in terms of the *dynamics-dependent displacement of peaks* to such lower field, as a novel means of probing the dynamic aspect of membrane protein. Namely, the transmembrane $\alpha_{\rm II}$-helix could be ascribed to a residue whose time-averaged deviation of torsion angles of the peptide unit at ambient temperature differs from that of static ones available at low temperature. The carbonyl ^{13}C peaks, on the other hand, are not sensitively displaced by such local anisotropic fluctuations, because they are more sensitive to the manner of hydrogen bond interactions.

Third, it is notable that the ^{13}C NMR signal of Ala 184 at ambient temperature (Fig. 2) is resonated at the extraordinary lower field at the peak-position of the loop region (17.27 ppm) [18] than the expected peak-position (higher than 16.88 ppm as boundary peak) as a residue located at the transmembrane α-helix F deduced by the diffraction data at cryo-temperature [9–12]. To discuss this issue in more detail, unambiguous assignment of this peak was made by recording the ^{13}C NMR spectrum of [3-^{13}C]Ala-A184G mutant with reference to that of wild type under the condition that several superimposed ^{13}C NMR signals of Ala residues located near at the membrane surfaces (Ala 160, 103, 235) were completely removed by accelerated spin relaxation rate due to addition of 40 μM Mn^{2+} ion [18]. The experimental verification of this peak will be discussed later. It is expected that such anomalous behavior of the ^{13}C chemical shift arises from the presence of highly distorted torsion angles at the peptide unit of Ala 184, coupled with undergoing conformational fluctuations caused by the kinked structure at Pro 186 *at ambient temperature*. To support this view, such anomaly in the ^{13}C chemical shift is not any more seen for [3-^{13}C]Ala-labeled P186A mutant which mimics dynamic conformation of bR at low temperature [18].

It is emphasized that molecular motions of intermediate frequency, if any, with time scale of 10^{-5} s which can interfere with proton-decoupling frequency (ca. 50 kHz) can be very easily detected when certain ^{13}C NMR signals both from CP-MAS and DD-MAS NMR spectra of [3-^{13}C]Ala-labeled bR or mutants were simultaneously suppressed [26]. Such motion was first recognized when ^{13}C NMR signals of the above-mentioned C-terminus of bR were almost completely suppressed at lower temperature at temperatures below $-40^{\circ}C$ or relative humidity lower than 86% [3]. This kind of peak suppression is also present at ambient temperature for loops and some transmembrane helices of bacterioopsin (bO) or several mutants of bR [17]. Further, molecular motions with correlation times in the order of 10^{-4} s, if any, could interfere with magic angle spinning in the order of 4 kHz and result in suppression of loop signals of [1-^{13}C] or [2-^{13}C]Ala-bR [13]. Therefore, it turned out that bR structure at ambient temperature as revealed by the current ^{13}C NMR data is not rigid as anticipated from the diffraction data at low temperature but dynamically heterogeneous undergoing motional fluctuations of various ranges of frequencies (or correlation times as reciprocal numbers) [3,13,17], as schematically illustrated in Fig. 4.

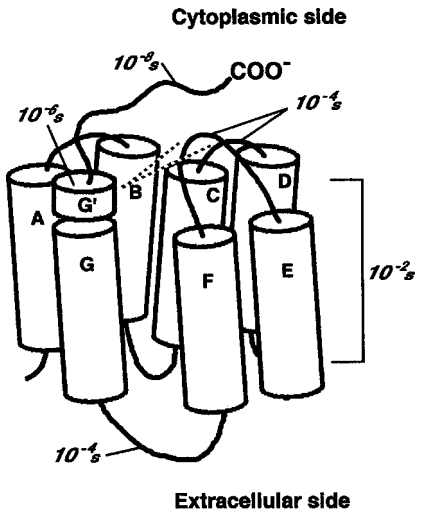

Fig. 4. Dynamic picture of bacteriorhodopsin undergoing fluctuation with various correlation times, as revealed by ^{13}C NMR. The C-terminal α-helix protruded from the membrane surface is designated by the helix G′ and mutual interaction with the helix G′ and C–D and E–F loops are indicated by the dotted lines.

Undoubtedly, this kind of dynamic picture for membrane proteins seems to be essential to exhibit a variety of biological functions effectively.

4. Long-distance interaction among residues for information transfer

As demonstrated already, it appears that long range interaction between the extracellular side and cytoplasmic side triggered by photoisomerization of retinal plays important role as proton pump. Such long distance information transfer could be mediated by a possible local conformational as well as dynamics changes of related amino-acid residues through helix–helix or side–chain interactions, if any. To this end, Tanio et al. recorded ^{13}C NMR spectra of [1-^{13}C]Val labeled wild type and V49A, V199A, T46V, T46V/V49A, D96N and D85N mutants to study conformational changes of the backbone caused by site-directed mutations along the extracellular surface and the cytoplasmic half channel [21]. In particular, they showed that there appears to be coupling between Val 49 and Asp 85 and between Asp 85 and Glu 204.

As illustrated in Figs 5 and 6, it is also possible to examine how local conformational changes of remote residues in the inner part of the transmembrane α-helices, for instances, at either Ala 81, 84 (he-

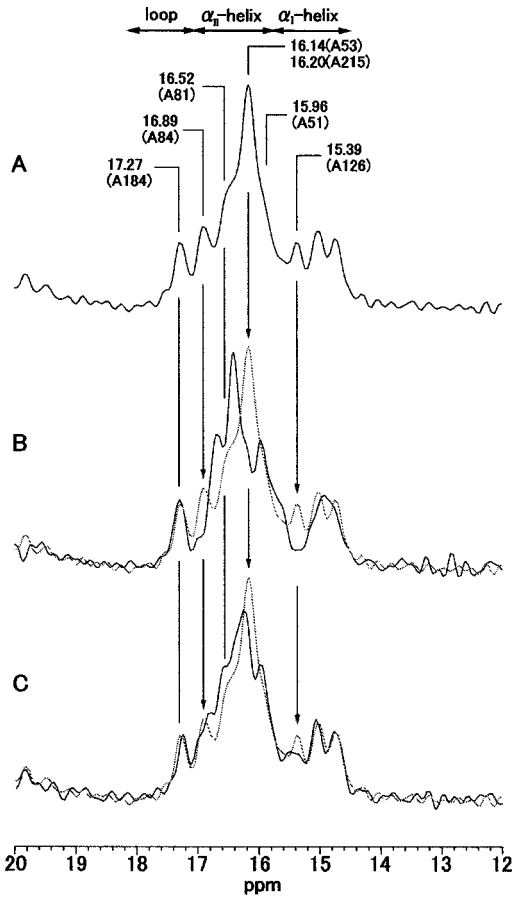

Fig. 5. ^{13}C CP-MAS NMR spectra of [3-^{13}C]Ala-labeled wild type (A), E204Q (B) and E204D (C) mutants. All spectra were recorded in the presence of 40 μM Mn^{2+} ion. Dotted spectra in the traces B and C are from 40 μM Mn^{2+}-treated wild type.

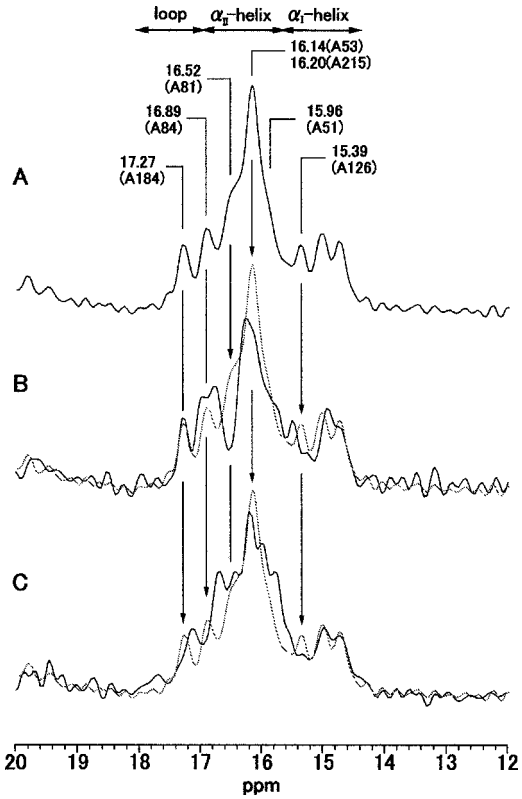

Fig. 6. ^{13}C CP-MAS NMR spectra of [3-^{13}C]Ala-labeled wild type (A), E194Q (B) and E194D (C) mutants. All spectra were recorded in the presence of 40 μM Mn^{2+} ion. Dotted spectra in the traces B and C are from 40 μM Mn^{2+}-treated wild type.

lix C), 53, 51 (helix B), or 215 (helix G) residues whose relative locations can be visualized based on recent X-ray diffraction data in Fig. 7 [11], are altered by replacement of one of the proton release group such as Glu 204 and 194 with Gln and Asp, respectively, to mimic protonation, as viewed from their Mn^{2+}-treated ^{13}C NMR spectra, respectively. In these spectra, superimposed ^{13}C NMR signals of [3-^{13}C]Ala-residues located near at the surface are removed by selective line-broadenings due to the accelerated spin-relaxations. Clearly, distinct local conformational changes are found to be induced at the site of Ala 53, 84, 126 and 215 located at the vicinity of Asp 85 in E204Q mutant (Fig. 5B), although no spectral change was induced at the vicinity of Ala 81, 51 and 184. E204D mutant exhibited more localized and smaller perturbation to Ala 53 and 215. Distinct spectral change at Ala 84 is still distinguishable (Fig. 5C). This means that site-directed mutation at the side-chain of E204 induced local conformational changes near at retinal (as viewed from Ala 53 and 215) and proton channel (as viewed from the effect of Asp 85) and this effect is more prominent in the E204Q mutant. In contrast, conformational change at Ala 81 is distinct for E194Q mutant but not detectable for E194D (Fig. 6B and 6C). Further, local conformational change is obvious at Ala 184 and 84 for E194D, although they are not distinct for E194Q mutant. It is therefore concluded that reduced side-chain lengths resulted in conformational changes in Ala 184 of helix F and Ala 126 of helix C. In other word, shortened chain length in the side chain of Glu 194 induced conformational changes of Ala 184 located at helix C as well as Ala 84 of helix F and Ala 126 of helix D.

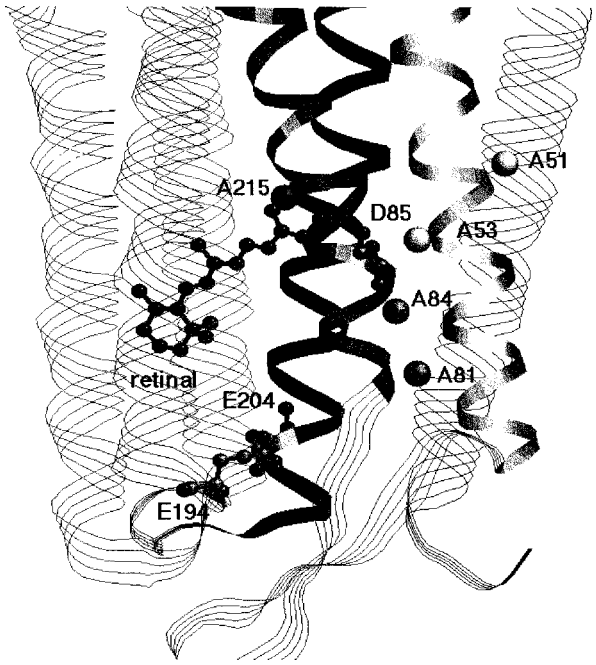

Fig. 7. Relative locations of Ala residues whose peaks are changed by mutations of side-chains in E204 and E194 shown upon the 3D structures of bacteriorhodopsin [11].

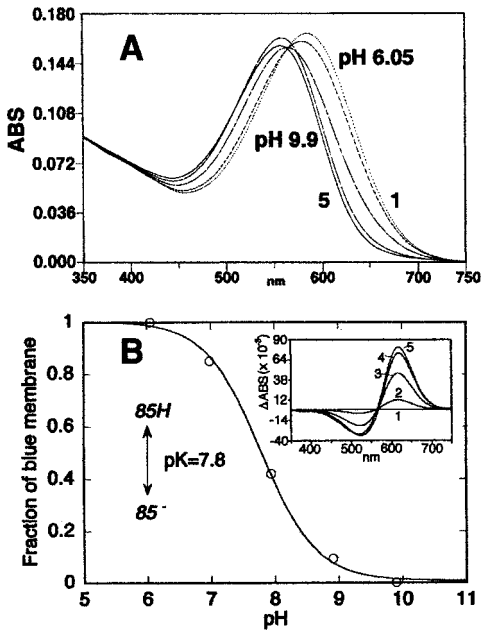

Fig. 8. pH dependence of the diluted suspension of R82Q mutant from pH 6.05 (dotted line; curve 1) to pH 9.9 (solid line; curve 5) (A). Their difference absorption spectra between pH 6.05–10 is illustrated in the inset of panel (B).

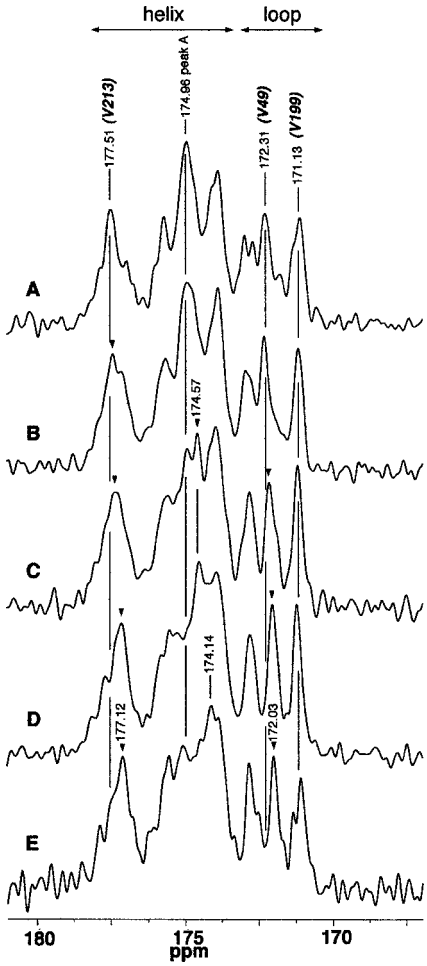

Fig. 9. pH change of ^{13}C CP-MAS NMR spectra of [1-^{13}C]Val-labeled R82Q mutant. A, B, C, D and E are corresponding to pH 6, 7, 8, 9 and 10.

It seems to be very important to reveal how the above-mentioned protonation signal at Asp 85 can be transmitted to remote residues at either extracellular or cytoplasmic sides of bacteriorhodopsin, with emphasis upon revealing a possible involvement of Arg 82 and Thr 89. To this end, it is more preferable to utilize R82Q mutant with pK_a 7.2, responsible for protonation at Asp85, instead of wild type with pK_a ca. 2.5 [27]. In fact, the absorption maximum of dark-adapted R82Q is shifted from 588 nm (blue form) at pH 6 to 552 (purple form) at pH 10 by raising pH (Fig. 8). Therefore, we examined pK_a responsible for protonation of Asp 85 by recording the difference spectrum at 618 nm, corresponding to the blue to purple transition, as 7.8 in the presence of 10 mM NaCl. In accordance with this change, the ^{13}C NMR signals of Val 213 and Val 49 (as indicated by the wedges) of [1-^{13}C]Val-labeled R82Q mutant seem to be appreciably displaced upfield by raising pH, owing to induced local conformational changes as viewed from these residues, as shown in Fig. 9. The apparent pK_a for R82Q as determined by a plot of displaced Val 213 and 49 residues in R82Q mutant against pH is 8.3 and 8.2, respectively, which is close to that of 7.8 for Asp 85 as demonstrated in Fig. 10 and coupled with the charged state of Asp 85. In contrast, pK_a value of wild type is 8.8 as viewed from the displacement of ^{13}C NMR signal of Val 49 (spectrum not

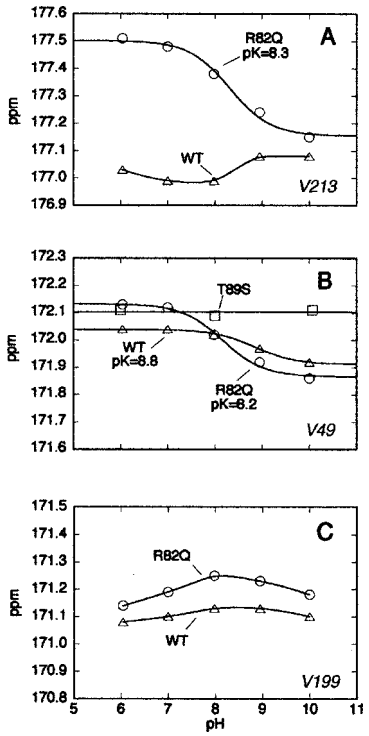

Fig. 10. Plots of ^{13}C NMR peaks of Val 213 (A), Val 49 (B) and Val 199 (C) in R82Q (circles), T89S (square) and WT (triangles) against pH.

shown) in spite of pK_a 7.8 from the absorption spectra and seemed to be coupled with an unidentified amino acid residue via interaction with Thr 89. In fact, there appears no pH-dependent change in the pH-titration study for T89S mutant (Fig. 10). This means that these induced local conformational changes at helices B and G are strongly influenced by the deprotonated state of Asp 85 in R82Q. The slight differences in these pK_a's in the latter, however, may be ascribed to a possible involvement of the side-chain methyl group in Thr 89 (helix C) of R82Q mutant, because no such pK_a deviation was anymore noted between the protonation state of Asp 85 (7.0) and the conformational changes in Val 49 (6.9) and Val 213 (7.1) of R82Q/T89S mutant (spectra not shown) (Fig. 11). In other word, the evidence of backbone conformational and fluctuational changes mediated by reduced interactions among helices B, C and G, and by structural change of the side chains of Arg 82, both of which are induced by the protonation of Asp85. Such structural and fluctuation changes would cause long-distance effects between the cytoplasmic and extracellular surface regions and regulation of the pK_a of internal amino acids in bR, as in the lowered pK_a of Asp 96 in D85N [28].

5. Concluding remarks

We have demonstrated that the current ^{13}C NMR approach on [3-^{13}C]Ala or [1-^{13}C]Val-labeled bacteriorhodopsin can be an excellent tool to gain insight into their conformational and dynamic aspects with emphasis on revealing their surface structures which are in many instances unavailable from diffraction studies. Dynamic picture of bR turned out to be not static at ambient temperature as anticipated from

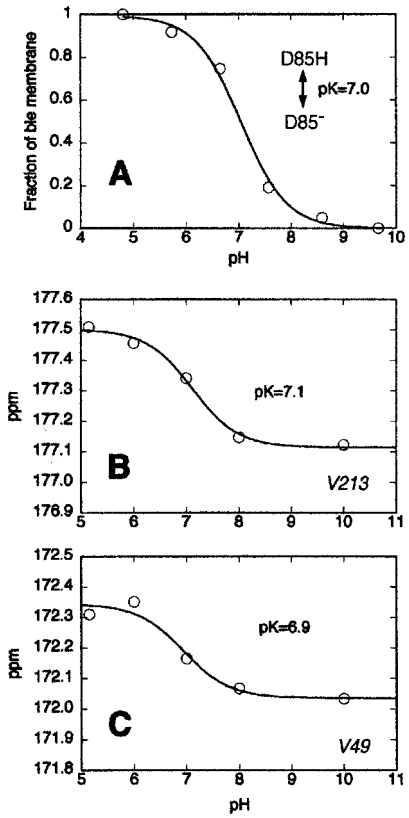

Fig. 11. (A): pH dependent absorption changes at 620 nm of the diluted R82Q/T89S mutants. (B) and (C): Plots of ^{13}C NMR peaks of Val 213 (B) and 49 (C) against pH.

crystalline sample obtained at cryo-temperature but very flexible, especially at the surface residue. It was shown that a long distance interaction among key residues was found to play an important role to exhibit effective proton pump activity through their backbone and/or side-chain interactions. Further, it is emphasized that this kind of flexible structure plays a very important role in exhibiting a variety of biological functions.

References

[1] S.J. Opella, P.L. Stuart and K.G. Valenntine, Protein structure by solid-state NMR spectroscopy, *Q. Rev. Biophys.* **19** (1987), 7–49.
[2] R. Fu and T.A. Cross, Solid-state nuclear magnetic resonance investigation of protein and polypeptide structure, *Annu. Rev. Biophys. Biomol. Struc.* **28** (1999), 235–268.
[3] H. Saitô, M. Tanio, S. Tuzi and A. Naito, Dynamic aspect of membrane proteins and membrane-associated peptides as revealed by ^{13}C NMR: Lessons from bacteriorhodopsin as an intact protein, *Annu. Rep. NMR Spectrosc.* **47** (2002), 39–108.
[4] J.K. Lanyi, Proton translocation mechanism and energetics in the light-driven pump bacteriorhodopsin, *Biochim. Biophys. Acta* **1183** (1993), 241–246.
[5] M.S. Braiman, T. Mogi, T. Marti, L.J. Stern, H.G. Khorana and K.J. Rothchild, Vibrational spectroscopy of bacteriorhodopsin mutants: light-driven proton transport involves protonation changes of aspartic acid residues 85, 96, and 212, *Biochemistry*, **27** (1988), 8516–8520.

[6] L.S. Brown, J. Sasaki, H. Kandori, A. Maeda, R. Needleman and J.K. Lanyi, Glutamic acid 204 is the terminal proton release group at the extracellular surface of bacteriorhodopsin, *J. Biol. Chem.* **270** (1995), 27 122–27 120.
[7] A.K. Dioumaev, H.T. Richter, L.S. Brown, M. Tanio, S. Tuzi, H. Saitô, Y. Kimura, R. Needleman and J.K. Lanyi, Existence of a proton transfer chain in bacteriorhodopsin: participation of Glu-194 in the release of protons to the extracellular surface, *Biochemistry* **37** (1998), 2496–2506.
[8] L.S. Brown, Y. Gat, M. Scheves, Y. Yamazaki, A. Maeda, R. Needleman and J. K. Lanyi, The retinal Schiff base-counterion complex of bacteriorhodopsin: changed geometry during the photocycle is a cause of proton transfer to aspartate 85, *Biochemistry* **33** (1994), 12 001–12 011.
[9] N.T. Grigorieff, A. Ceska, K.H. Downing, J.M. Baldwin and R. Henderson, Electron crystallographic refinement of the structure of bacteriorhodopsin, *J. Mol. Biol.* **259** (1996), 393–421.
[10] P.E. Pebay-Peyroula, G. Rummel, J.P. Rosenbusch and E.M. Landau, X-ray structure of bacteriorhodopsin at 2.5 angstroms from microcrystals grown in lipidic cubic phases, *Science* **277** (1997), 1676–1681.
[11] H. Luecke, H.T. Richter and J.K. Lanyi, Proton transfer pathways in bacteriorhodopsin at 2.3 angstrom resolution, *Science* **280** (1998), 1934–1937.
[12] L.O. Essen, R. Siegert, W.D. Lehmann and D. Oesterhelt, Lipid patches in membrane protein oligomers: crystal structure of the bacteriorhodopsin–lipid complex, *Proc. Natl. Acad. Sci. USA* **95** (1998), 11 673–11 678.
[13] S. Yamaguchi, S. Tuzi, K. Yonebayashi, A. Naito, R. Needleman, J.K. Lanyi and H. Saitô, Surface dynamics of bacteriorhodopsin as revealed by ^{13}C NMR studies on [^{13}C]Ala-labeled proteins: Detection of millisecond or microsecond motions in interhelical loops and C-terminal α-helix, *J. Biochem. (Tokyo)* **129** (2001), 373–382.
[14] H. Saitô, Conformation-dependent ^{13}C chemical shifts: A new means of conformational characterization as obtained by high-resolution solid-state 13C NMR, *Magn. Reson. Chem.* **24** (1986), 835–852.
[15] H. Saitô and I. Ando, High-resolution solid-state NMR studies of synthetic and biological macromolecules, *Annu. Rep. NMR Spectrosc.* **21** (1989), 209–290.
[16] H. Saitô, S. Tuzi and A. Naito, Empirical versus nonempirical evaluation of secondary structure of fibrous and membrane proteins by solid-state NMR: A practical approach, *Annu. Rep. NMR Spectrosc.* **36** (1998), 79–121.
[17] H. Saitô, S. Tuzi, S. Yamaguchi, M. Tanio and A. Naito, Conformation and dynamics of bacteriorhodopsin revealed by ^{13}C NMR, *Biochim. Biophys. Acta* **1460** (2000), 39–48.
[18] S. Tuzi, J. Hasegawa, R. Kawaminami, A. Naito and H. Saitô, Regio-selective detection of dynamic structure of transmembrane α-helices as revealed from ^{13}C NMR spectra of [3-^{13}C]Ala-labeled bacteriorhodopsin in the presence of Mn^{2+} ion, *Biophys. J.* **81** (2001), 425–434.
[19] S. Yamaguchi, K. Yonebayashi, H. Konishi, S. Tuzi, A. Naito, J. K. Lanyi, R. Needleman and H. Saitô, Cytoplasmic surface structure of bacteriorhodopsin consisting of interhelical loops and C-terminal α-helix, modified by a variety of environmental factors as studied by ^{13}C NMR, *Eur. J. Biochem.* **268** (2001), 2218–2228.
[20] S. Tuzi, A. Naito and H. Saitô, A high-resolution solid-state ^{13}C NMR study on [1-^{13}C]Ala and [3-^{13}C]Ala and [1-^{13}C]Leu and Val-labelled bacteriorhodopsin, *Eur. J. Biochem.* **218** (1993), 837–844.
[21] M. Tanio, S. Inoue, K. Yokota, T. Seki, S. Tuzi, R. Needleman, J.K. Lanyi, A. Naito and H. Saitô, Long-distance effects of sie-directed mutations on backbone conformatin in bacteriorhodopsin from solid state NMR of [1-^{13}C]Val-labeled proteins, *Biophys. J.* **77** (1999), 431–442.
[22] S. Tuzi, A. Naito and H. Saitô, A ^{13}C NMR study on conformation an dynamics of the transmembrane α-helices, loops and C-terminus of [3-^{13}C]Ala-labeled bacteriorhodopsin, *Biochemistry* **33** (1994), 15 046–15 052.
[23] S. Yamaguchi, S. Tuzi, T. Seki, M. Tanio, R. Needleman, J.K. Lanyi, A. Naito and H. Saitô, Stability of C-terminal α-helical domain of bacteriorhodopsin protruding from the membrane surface as studied by high-resolution solid-state ^{13}C NMR, *J. Biochem. (Tokyo)* **123** (1998), 78–86.
[24] S. Kimura, A. Naito, S. Tuzi and H. Saitô, A ^{13}C NMR study on [3-^{13}C]-, [1-^{13}C]Ala- or [1-^{13}C]Val-labeled transmembrane peptides of bacteriorohodopsin in lipid bilayers: Insertion, rigid-body motions, and local conformational fluctuations at ambient temperature, *Biopolymers* **58** (2001), 78–88.
[25] S. Krimm and A.M. Dwivedi, Infrared spectrum of the purple membrane: Clue to proton conduction mechanism?, *Science* **216** (1982), 407–408.
[26] W.T. Rothwell and J.S. Waugh, Transverse relaxation of dipolar coupled spin system under rf irradiation: detecting motions in solid, *J. Chem. Phys.* **75** (1981), 2721–2732.
[27] L.S. Brown, Y. Gat, M. Sheves, Y. Yamazaki, A. Maeda, R. Needleman and J.K. Lanyi, The retinal Schiff base-counterion complex of bacteriorhodopsin: changed geometry during the photocycle is a cause of proton transfer to aspartate 85, *Biochemistry* **33** (1994), 12 001–12 011.
[28] Y. Kawase, M. Tanio, A. Kira, S. Yamaguchi, S. Tuzi, A. Naito, M. Kataoka, J.K. Lanyi, R. Needleman and H. Saitô, Alteration of conformation and dynamics of bacteriorhodopsin induced by protonation of Asp 85 and deprotonation of Schiff base as studied by ^{13}C NMR, *Biochemistry* **39** (2000), 14 472–14 480.